ACS OMEGA

http://pubs.acs.org/journal/acsodf

Article

Nanobacterial Cellulose Production and Its Antibacterial Activity in Biodegradable Poly(vinyl alcohol) Membranes for Food Packaging Applications

Manu L. Naik, Ashok M. Sajjan,* Ashwini M, Sharanappa Achappa, T. M. Yunus Khan, Nagaraj R. Banapurmath, Prakash B. Kalahal, and Narasimha H. Ayachit

Cite This: *ACS Omega* 2022, 7, 43559−43573

Read Online

ACCESS | Metrics & More | Article Recommendations | Supporting Information

ABSTRACT: Nanobacterial cellulose (NBC) was produced and incorporated into biodegradable poly(vinyl alcohol) (PVA) in different weight ratios to obtain polymer nanocomposite membranes. The physicochemical properties of the membranes were studied using Fourier transform infrared (FTIR) spectroscopy, a universal testing machine (UTM), thermogravimetric analysis (TGA), wide-angle X-ray diffraction (WAXD) techniques, and field emission scanning electron microscopy (FESEM). FTIR confirmed the consolidation of NBC into PVA by exhibiting significant changes in the peaks compared to NBC and PVA individually. The highest tensile strength of 53.33 MPa and 235.30% elongation at break of the membrane M-10 mass % NBC was obtained, illuminating that NBC provides stiffness and PVA imparts elasticity. WAXD revealed that the crystalline nature of the membrane increases up to 10 mass % and decreases beyond it. The effect of NBC on the poly(vinyl alcohol) membranes for food packaging was investigated systematically. Among all the membranes, M-10 mass % NBC was found to be the most suitable for packaging applications. Membranes had antimicrobial activity against food microbes and showed degradability behavior in the soil. The tests on membranes for packaging revealed that fruits were protected from spoilage caused by microorganisms. Hence, the prepared membranes could be used as an alternative to conventional plastics for packaging applications.

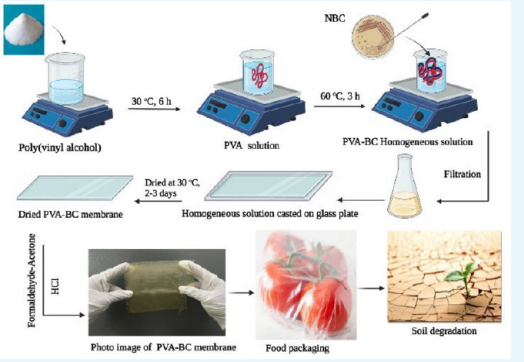

INTRODUCTION

Plastic is a synthetic material that is a significant threat to the environment in the present scenario.[1] The increasing demand for packaging has led to an immense amount of single-use plastic production and global plastic production rates. In recent years, the plastic production rate has been enhanced by approximately 360 million metric tonnes.[2] The average yearly consumption of plastics in India, as reported by the central pollution control board, is around 8 million tons, which gets accumulated in nature, as it is devoid of degradation.[3] Increased consumption of nonbiodegradable plastic at an alarming rate has provided an opportunity to think in the direction of natural and biodegradable polymers.[4] According to the Japanese Biodegradable Polymer Society, biodegradable polymers (BPs) are conventional plastics that can be used for various purposes and decompose to water and carbon dioxide by the action of microorganisms when disposed of in a natural environment without excreting any toxic substances into nature.[5] Further, they show other properties such as mechanical strength, thermal stability, and water barrier properties due to additives.[6,7] Cellulose, poly(vinyl alcohol), starch, poly(caprolactone), poly(butylene succinate), and chitosan are some of the BPs used in the production of membranes for packaging applications.[8−10] Cellulose is copious, opulent, and readily available, but it has disadvantages due to its impurities such as pectin, lignin, and hemicelluloses, which increase the cost of production.[11] It is unsuitable for food packaging applications, as it does not possess antimicrobial properties.[12−16]

Food packaging applications play a important role in maintaining the quality of food and protecting it from the external environment for storage and transportation applications.[17,18] The polymer membranes used in food packaging should protect food from external factors such as moisture content, heat, microorganisms, microbial enzymes, light, contaminants, insects, dust particles, and harmful gaseous emissions.[11] They should also enhance the shelf life and quality of the food for a longer period to enhance the food packaging properties.[19] BPs incorporated with some of the antimicrobial agents or polymers exhibit the antimicrobial property that

Received: July 9, 2022
Accepted: November 3, 2022
Published: November 17, 2022

helps in protection from microbial contamination and has been used widely.[20] Zwitterionic polymers and nanomaterials such as silver nanoparticles, chlorine dioxide, graphene oxide, zeolite, triclosan, and quaternary ammonium compounds are some materials that have exhibited antimicrobial properties.[21−23] On the other hand, carbon-based nanomaterials, zwitterionic polymers, and metallic nanoparticles possess disadvantages that may restrict their functionality or cause environmental consequences.[24,25] As a result, there is a significant need for nanomaterials with antimicrobial activity that are ecologically friendly, affordable, and facile to fabricate on a wider scale.

Cellulose nanocrystals (CNCs) have excellent properties such as biodegradability, optical transparency, anisotropy, low density, elasticity, degree of polymerization, good tensile strength, high wet uptake capacity, and three-dimensional ultrafine coherent network and have drawn much attention.[26−31] Apart from these characteristics, CNCs possess an adjustable surface chemistry to meet specific demands by tailoring the physicochemical properties due to their high aspect ratio, stiffness, and abundance of functional groups containing oxygen. CNCs can potentially be used as a new class of antimicrobial agent in the membrane matrix for the development of antimicrobial membranes for food packaging.[32−35] Tyagi et al. reported that CNCs possess narrow and rigid characteristics and are able to inactivate microorganisms by puncturing the microbial cell membrane when they are incorporated into tissue paper, resins, paints, and packaging materials.[35] Noronha et al. studied the toxic effect of NBC on *Escherichia coli* cells when it was dispersed on a coated surface and in water. CNC-coated surfaces can inactivate approximately 90% of the attached *Escherichia coli* cells, confirming the potential of the CNCs to be applied as sustainable and cost-effective antibiofouling nanomaterials.[36]

PVA is a biodegradable, semicrystalline, nontoxic, biocompatible, water-soluble, less expensive, and prominent nonpetroleum synthetic polymer.[37−43] It has excellent tensile strength, miscibility, and film-forming ability; apart from its excellent properties, it has a few disadvantages such as poor decomposition temperature and low elongation at break. The disadvantages can be overcome by blending with another biopolymer.[44−46] The presence of hydroxyl groups of the PVA will establish hydrogen bonds with bacterial cellulose (BC) and acetal linkages with aldehydes. BC−PVA-based composites have been developed previously.[47−49] In this context, BC is a natural, renewable raw material synthesized as an extracellular protective layer with a thick white gelatinous pellicle formed at the air−liquid interface.[43] BC is a multifaceted biopolymer with versatile and unique properties compared with plant-derived cellulose in both wet and dry states.

An exhaustive literature survey found that BC does not possess antimicrobial properties but that cellulose nanocrystals prepared from plant cellulose exhibit antimicrobial properties due to the sharp edges of CNCs, which exhibit physical stress on the surface of microorganisms.[36]

Extensive literature surveys have been carried out on the production of nanobacterial cellulose and its antimicrobial property in PVA for food packaging applications. However, the production of NBC having antimicrobial properties has not been investigated. Hence, in the current research, an effort has been made to produce a novel NBC exhibiting antimicrobial properties using indigenously isolated microorganisms. Accordingly, NBC producing strain was isolated, screened, and molecularly characterized. Further, the produced NBC with different mass percents was incorporated in PVA to develop polymer nanocomposite membranes using a solution casting technique. The physicochemical properties of the prepared membranes were analyzed using FTIR, WAXD, TGA, FESEM, and mechanical properties. Water barrier properties such as water vapor transmission rate (WVTR), moisture retention capability (MRC), membrane solubility (MS), and swelling measurement of the membranes were tested. Antimicrobial activity, degradation, and food packaging tests were also performed to assess the efficiency of the PVA-NBC nanocomposite membranes for food packaging applications.

EXPERIMENTAL SECTION

Materials. Poly(vinyl alcohol) with an average molecular weight of ∼104500 (degree of hydrolysation 86−89%), isopropanol, formaldehyde, and disodium hydrogen phosphate (Na_2HPO_4) were purchased from s.d. fine-chemicals limited, Mumbai, India. Yeast extract and potassium chloride (KCl) were obtained from Sisco Research Laboratories, Mumbai, India, citric acid and magnesium sulfate ($MgSO_4$) were purchased from Qualigens fine chemicals, Mumbai, India, and carboxy-methylcellulose (CMC) was purchased from Sigma-Aldrich Chemicals. Peptone, glucose, and agar powder were purchased from HiMedia Laboratories Pvt. Ltd., Mumbai. Dipotassium hydrogen phosphate (K_2HPO_4) was obtained from Kemphasol Pvt. Ltd., Mumbai. Sodium nitrate ($NaNO_3$), hydrochloric acid (HCl), and acetone were purchased from Rankem RFCL Limited, New Delhi. All of the chemicals were of reagent grade and were used without further purification. Double-distilled water was used for the study.

Sample Collection. Soil samples were collected near water bodies at various agricultural fields at Hanchali, Vijayapura, and Karnataka, India and used to isolate and screen potential NBC producers. Soil samples were collected in a sterile bottle and stored at 4 °C.[50]

Isolation of Nanobacterial Cellulose Producing Bacteria. Enrichment of the soil sample was done by inoculating 5 g of sample into a 250 mL flask containing 95 mL of CMC media (CMC 5 g/L, sodium nitrate 2 g/L, dipotassium phosphate 1 g/L, magnesium sulfate 0.5 g/L, potassium chloride 0.5 g/L, and peptone 0.5 g/L) maintained at pH 7 which was sterilized at 121 °C for 15 min. After inoculation, the flask was incubated in an incubator shaker at 35 °C for 48 h. After incubation, 1 mL of enrichment broth was subjected to serial dilution and later spread plated on Hestrin−Schramm (HS) agar media (glucose 20 g/L, yeast extract 5 g/L, peptone 5 g/L, dipotassium phosphate 2.7 g/L, citric acid 1.15 g/L, and agar 15 g/L) at pH 7 and incubated at 35 °C.[50]

Screening of Nanobacterial Cellulose-Producing Bacteria. After serial dilution of enrichment media as stated in the procedure above, 1 mL of 10^{-6} serially diluted media was spread on HS agar media and incubated at 35 °C for 24 h. After incubation, different bacterial colonies grown on the HS agar plate were screened for NBC production by picking a loop full of the culture and inoculating it in a flask containing 100 mL of HS media. The flask was later incubated at 35 °C in an incubator shaker for 48 h and later at 35 °C in a static incubator for 6 days. After incubation, the flask containing cellulose-producing bacteria that formed a white pellicle at the air−liquid interface covering the surface of the liquid medium was selected. The flask with pellicle growth was selected and

https://doi.org/10.1021/acsomega.2c04336
ACS Omega 2022, 7, 43559−43573

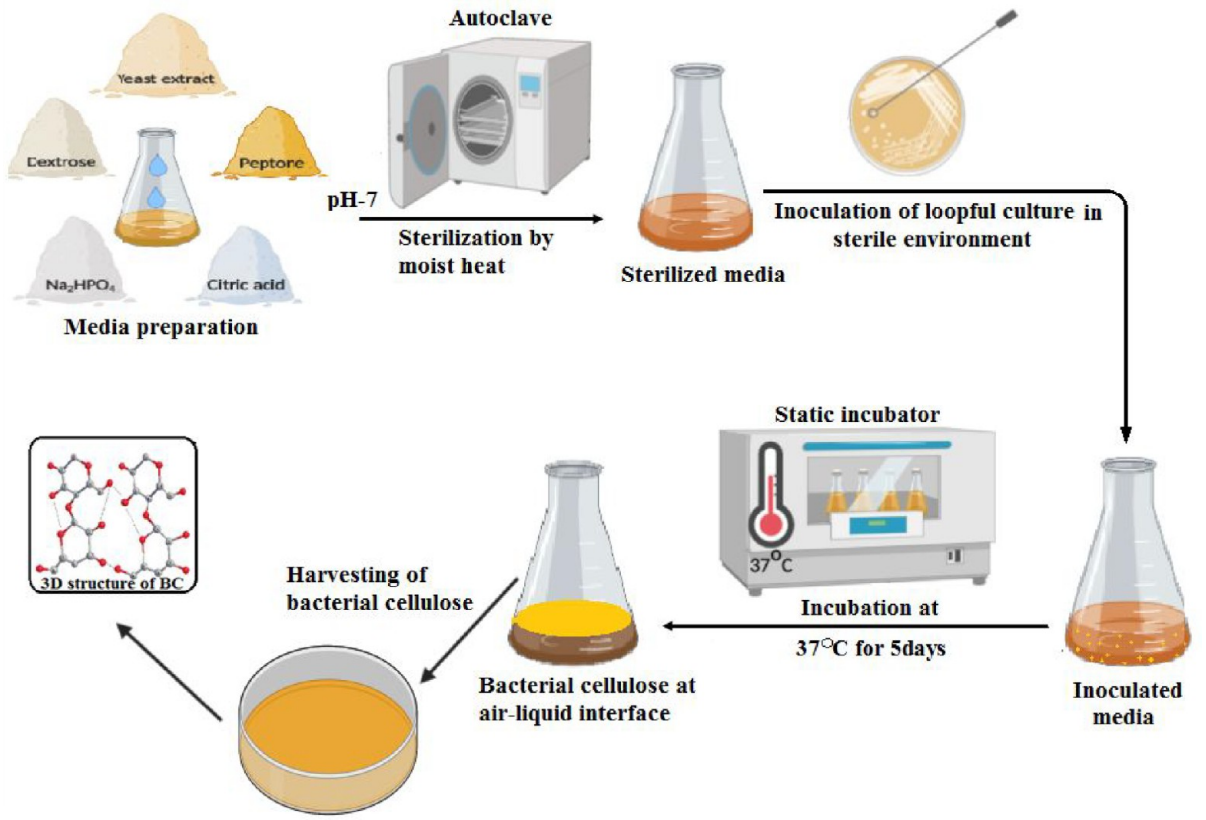

Figure 1. Flowchart for production of NBC.

purified by repeated streaking on HS agar plates to obtain isolated, purified cultures. Each distinct colony was further inoculated into 100 mL of HS media, and the bacterial strain (LRP1) with the highest production of NBC (based on dry weight) was selected for molecular characterization and NBC production.[51]

Molecular Characterization. Based on NBC production, the bacterial strain LRP1 was selected and was characterized by a molecular characterization method by the 16s rRNA gene. Specific primers 907R_704F were used to amplify genes. The genes were amplified by PCR and sequenced by Sanger methods with an ABI 3500XL genetic analyzer (Life Technologies, USA). After amplification, the gene was subjected to a search for homologous sequences from the National Centre for Biotechnology Information (NCBI) database using a tool called the nucleotide basic local alignment search tool (BLASTn) available from NCBI. A highly homologous sequence was selected, and a multiple sequence analysis was performed to deduce a phylogenetic tree using the molecular evolutionary genetic analysis (MEGA 6.0) tool. Phylogenetic analysis was used to characterize the isolated strain LRP1 based on the sequence similarity.[52]

Production of Nanobacterial Cellulose. A submerged fermentation (SmF) method was used to produce NBC, which was used as an antimicrobial additive to prepare antimicrobial membranes. Fermentation was carried out in a 250 mL conical flask containing 100 mL of HS media at pH 7. After the preparation of HS media, the fermentation flask was kept in an autoclave at 121 °C and 15 psi for 15 min for sterilization of the media. After sterilization, the fermentation flask was inoculated with a loopful of culture under sterile conditions in a laminar airflow. The fermentation flask was incubated in a static incubator at 35 °C for 8 days. Figure 1 shows the flowchart for the production of NBC. During incubation, the bacterial stain LRP1 produced cellulose in the form of a white pellicle at the air−liquid interface covering the surface of the liquid medium. Later, the white pellicle was picked, washed, dried, and used with PVA for membrane preparation.[53]

Membrane Preparation. Poly(vinyl alcohol) (6 g) was dissolved in 100 mL of deaerated distilled water with constant stirring for about 6 h at room temperature. The PVA solution was filtered and spread onto a glass plate with the help of a casting knife in a dust-free atmosphere. After casting, the PVA solution was allowed to dry for about 2−3 days at ambient temperature. The completely dried membrane was subsequently peeled off and designated as M-PVA. To prepare an NBC-incorporated PVA membrane, a known amount of a NBC suspension was prepared by adding a known amount of NBC to 30 mL of distilled water.[49] The suspension was stirred for 6 h at 60 °C followed by ultrasonication with a fixed frequency of 40 kHz (Anamatrix.in LMUC-3) for 30 min to reduce particle aggregation and enhance dispersion. The rest of the procedure was followed by a procedure similar to that for the M-PVA membrane. However, the amount of NBC suspension with respect to PVA was varied as 5, 10, 15, and 20 mass %, and the membranes thus obtained were designated as M-5 mass % NBC, M-10 mass % NBC, M-15 mass % NBC, and M-20 mass % NBC, respectively. The thickness of the membranes was measured at different points using a Peacock dial thickness gauge with an accuracy of ±2 μm. The thickness of the membranes was found to be 90 ± 2 μm.

All of the developed membranes were cross-linked using a formaldehyde−acetone solution by an immersion method. The membranes were immersed in a formaldehyde−acetone

https://doi.org/10.1021/acsomega.2c04336
ACS Omega 2022, 7, 43559−43573

solution containing 10% formaldehyde and 90% acetone by volume. To enhance the cross-linking reaction, the pH of the solution was maintained at around 1.00 by HCl.[54] After carrying out the cross-linking reaction for 1 min at room temperature, the partially cross-linked membranes were removed from the formaldehyde−acetone solution and rinsed with isopropanol followed by water to remove the residual formaldehyde and acetone. Further, membranes were dried at room temperature until their weights were constant and used for experiments.[55]

Membrane Characterization. The physicochemical properties of the developed membrane were characterized by different characterization techniques. The structural interaction between PVA and NBC was studied by Diamond ATR Fourier transform infrared (FTIR) spectroscopy (PerkinElmer Pvt. Ltd., 28, Ayer Rajah Crescent, Singapore). FTIR spectra were recorded in the range of 500−4000 cm^{-1}. A SZ-100 V2 series nanoparticle analyzer (Horiba Ltd., 2 Miyanohigashi, Kisshoin, Minami-ku Kyopto, Japan) was used to determine the particle size and ζ potential of the developed membrane. The crystalline nature of the PVA, NBC, and PVA-NBC composite membranes was determined using an X-ray diffractometer (WAXD, Phillips P.W. 1830 diffractometer, USA) equipped with nickel-filtered Cu Kα radiation and scanned in the reflection mode in a 2θ angle range of 5−80° at a speed of 8°/min.[56] Thermal analysis of the developed composite membranes was carried out using a thermogravimetric analyzer (Mettler-Toledo, USA) in a temperature range of 30−550 °C at a heating rate of 10 °C/min.[57] The mechanical strength and thickness were measured by using a universal testing machine (UTM) (Tinius Olsen, USA) and digimatic micrometer (Mitutoyo, USA), respectively. The water vapor transmission rate (WVTR) of the developed membrane was measured as per a reported procedure.[55] The moisture retention capability (MRC) of the developed membrane of dimensions 1 cm × 1 cm was determined by drying the samples in an oven at a specified temperature for a given period.[57−59] To confirm the hydrophilic nature of the developed membranes, a membrane-sorption analysis (swelling measurement) was conducted according to the procedure mentioned in a previous study.[60] The membrane solubility (MS) of the developed membranes was estimated using a wet method according to the procedure reported in a previous study.[60]

Antibacterial Activity Measurement. The antibacterial activities of the developed membranes were evaluated by the method of disk diffusion. The Gram-negative bacteria *Escherichia coli* (*E. coli*) and Gram-positive bacteria *Micrococcus luteus* (*M. luteus*), *Staphylococcus aureus* (*S. aureus*), and *Bacillus cereus* (*B. cereus*) were used as pathogens for testing. The pathogens were cultivated in nutrient broth (13 g/L) and incubated in a shaking incubator at 35 °C for 24 h. The pathogenic broth (100 μL) was inoculated to the nutrient agar plate (nutrient broth with 2 wt % of agar) and spread evenly using a glass spreader. A membrane sample 2 cm in diameter was loaded at the center of the plates. Later, the plates were kept in a static incubator at 35 °C for 24 h. The antibacterial activity was analyzed by measuring the zone of clearance in millimeters.

Packaging Ability. Fresh tomatoes were washed with water and dried to remove any dust particles. The experiment was carried out in triplicate, wherein eight tomatoes were used. Among these, four tomatoes were stored unpacked and the remaining four were packed using an M-10 mass % NBC membrane. The tomatoes were stored at a temperature of 25 ± 2 °C. The quality of both packaged and unpackaged tomatoes was evaluated every alternate day during storage.

Biodegradability Test. The degradation ability of the M-10 mass % NBC membrane was determined using soil burial tests at the laboratory level. A square sample was cut and weighed on the initial day. All samples were dried at 50 °C for 24 h before weighing. Container like mud-pot, wherein soil was added, and the membrane sample were placed in the soil at a depth of 10 cm from the surface. The soil was moistened daily with a sufficient water. The weight loss was determined every 10 days, where the membranes were washed with double-distilled water and dried in an oven at 50 °C for 24 h and the obtained weight was analyzed.

RESULTS AND DISCUSSION

Production and Screening of Nanobacterial Cellulose. The isolated strain LRP1 produced NBC with 2.5 g/L (dried weight) at the air−liquid interface. as shown in Figure 2.

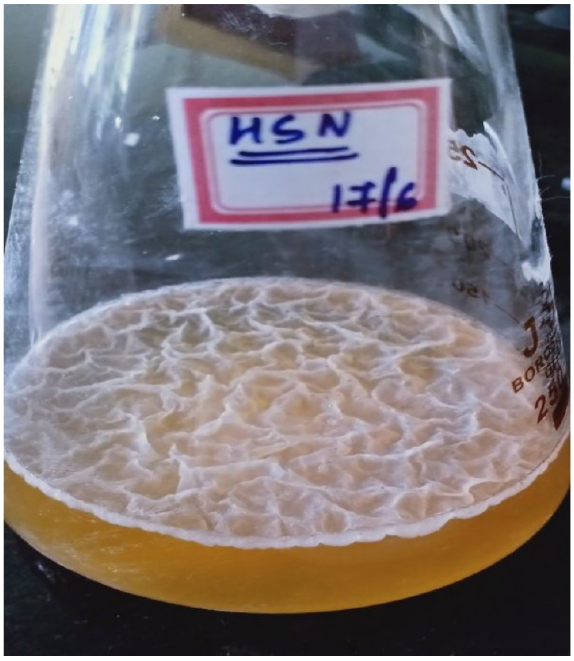

Figure 2. Nanobacterial cellulose at the air−liquid interface.

The harvested NBC was found to be thick and was floating on the surface of the media at the air−liquid interface.[51,52] Further, the selected strain LRP1 was molecularly characterized based on the 16s rRNA gene for specific primers 907R_704F. LRP1 was identified as *Bacillus subtilis* by 16s rRNA gene sequencing and a phylogenetic analysis.

Figure 3 shows the phylogenetic tree of LRP1, which showed the closest homology to the sequence of *Bacillus subtilis* strain IAM 12118 (accession id MK267098). However, the identified strain was designated *Bacillus subtilis* strain LRP1. The 16s rRNA sequence of isolated strain LRP1 was submitted and deposited with the NCBI database with accession no. ON287190.

Particle Size Distribution and ζ Potential Analyses. Figure 4 shows the hydrodynamic size distribution of the NBC in water analyzed in a zetasizer using the DLS technique. The hydrodynamic size of NBC was approximately 108 nm with respect to the histogram, as shown in Figure 4A. Further, to

https://doi.org/10.1021/acsomega.2c04336
ACS Omega 2022, 7, 43559−43573

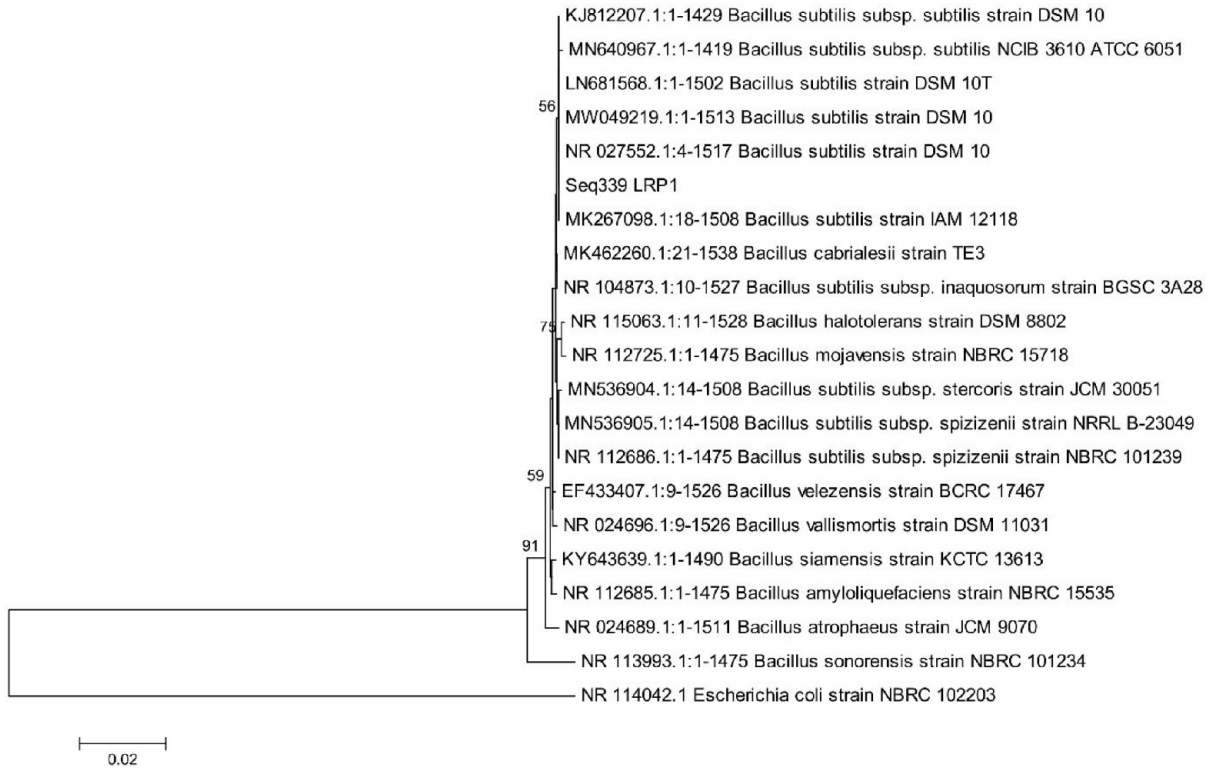

Figure 3. Phylogenetic tree of LRP1 isolate by MEGA6.

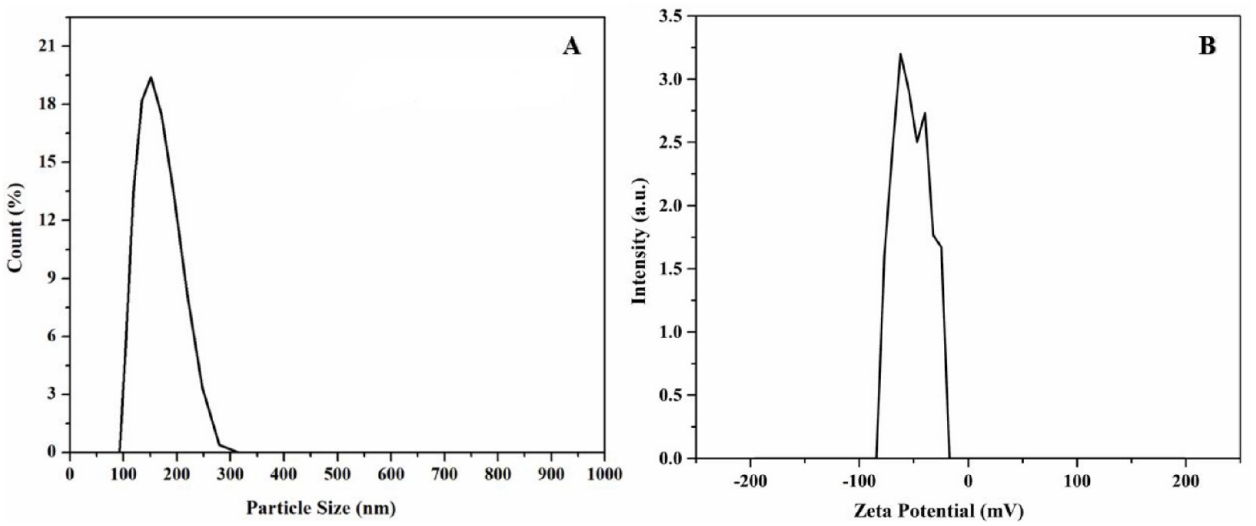

Figure 4. (A) Histogram of DLS and (B) ζ potential graph of NBC.

determine the physical stability, the ζ potential of colloidal dispersions of NBC was measured and found to be −53.6 mV, as shown in Figure 4B. These data suggested that NBC had excellent dispersity, a relatively narrow size distribution, and stability in an aqueous solution.

Wide-Angle X-ray Diffraction Analysis (WAXD). Figure 5A gives the X-ray diffractograms of NBC. The characteristic peak at $2\theta = 42.7°$ can be attributed to the crystalline nature of NBC.[56,61] The average crystallite size of the nanocrystalline cellulose was estimated according to the Debye−Scherrer equation[62]

$$D = k\lambda/\beta \cos\theta$$

where D is the average crystallite size, k is the particle shape factor, λ is the X-ray wavelength, β is the full width at half-maximum of the peak, and θ is the Bragg angle corresponding to the intense diffraction peak. Based on the intense diffraction peak of NBC, it was found that the average crystallite size of NBC is 113 nm.

The crystalline nature of the developed non-cross-linked membranes was estimated based on an X-ray diffractogram. Figure 5B illustrates that WAXD of pristine PVA (M) had a strong crystalline diffraction peak at $2\theta = 19.6°$, which indicates that the pristine M contains both amorphous and crystalline natures in the membrane matrix.[60−64] In membranes M-5 mass % NBC and M-10 mass % NBC, the intensity

https://doi.org/10.1021/acsomega.2c04336
ACS Omega 2022, 7, 43559−43573

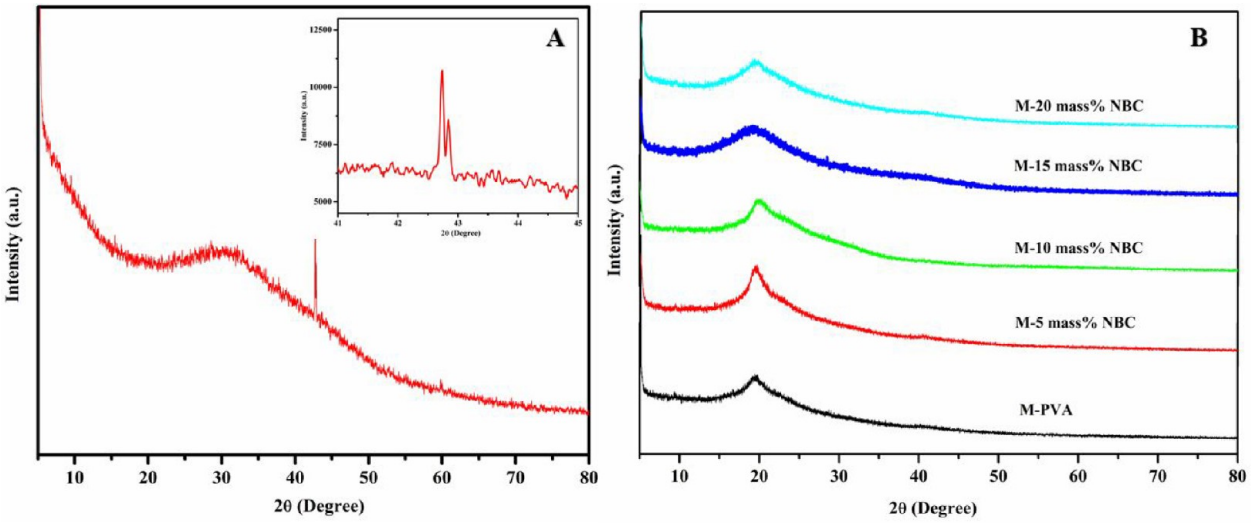

Figure 5. (A) WAXD analysis of NBC and of (B) the membrane M-PVA and cross-linked membranes M-5 mass % NBC, M-10 mass % NBC, M-15 mass % NBC, and M-20 mass % NBC.

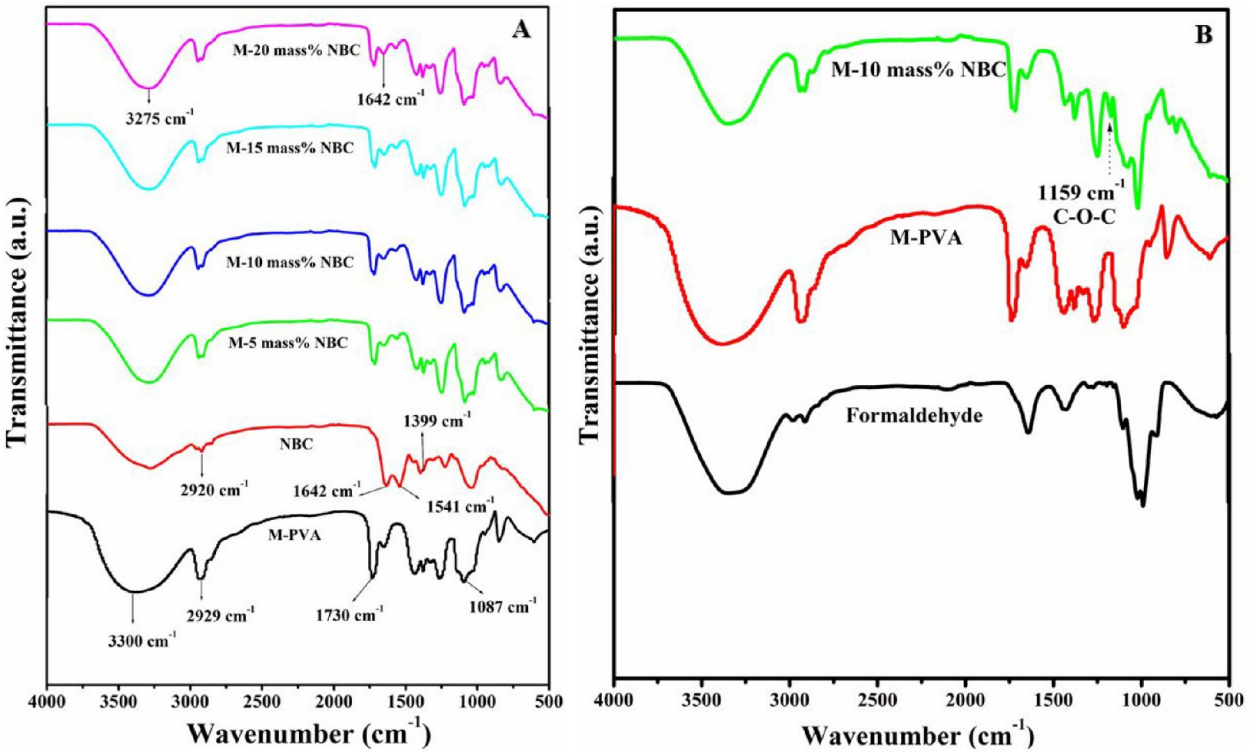

Figure 6. (A) FTIR spectra of membranes M-PVA, NBC, M-5 mass % NBC, M-10 mass % NBC, M-15 mass % NBC, and M-20 mass % NBC. (B) FTIR spectra of formaldehyde and M-PVA and cross-linked M-10 mass % NBC membranes.

found of the diffraction peak was enhanced at $2\theta = 20°$. This was due to the interaction between PVA and NBC, which results in the crystalline nature of the membrane. However, from membranes M-15 mass % NBC and M-20 mass% NBC, with the increase of NBC content in the M-15 mass % NBC membrane matrix, the intensity of the peak at $2\theta = 20°$ was found to gradually decrease. This indicated that the NBC content had an effect on the degree of crystallinity of the PVA membrane (M-15 mass % NBC and M-20 mass % NBC).[47]

Fourier Transform Infrared Spectroscopy (FTIR). Figure 6A shows the FTIR spectrum of the pristine PVA membrane (M-PVA), which depicts an inter- and intramolecular O−H stretching vibration at around 3300 cm^{-1} and C−O stretching vibrations illustrated by the presence of multiple absorption peaks appearing between 1000 and 1242 cm^{-1}. Peaks at 2929, 2853, 1730, and 1087 cm^{-1} correspond to C−H stretching, symmetric and asymmetric stretching from an alkyl group, C═O stretching, and C−O stretching, respectively.

The FTIR spectrum of pure NBC is shown in Figure 6A. The characteristic broad band at 3275 cm^{-1} corresponds to stretching vibrations of the O−H group.[65] The peak at 2920 cm^{-1} represents the aliphatic C−H stretching vibration. The peak at 1642 cm^{-1} is due to the deformation vibration of the

https://doi.org/10.1021/acsomega.2c04336
ACS Omega 2022, 7, 43559−43573

absorbed water molecules. Further, the peaks at 1541 and 1399 cm^{-1} were due to C−C stretching and ring vibrations. The peak at 1064 cm^{-1} could be associated with an ether C−O−C stretching vibration.[47,60−66]

FTIR spectra of all the NBC-incorporated PVA membranes are illustrated in Figure 6A. As the NBC mass percent in the PVA membrane increases, the intensity of hydroxyl group (O−H) stretching vibrations decreases along with a slight shift to lower wavenumber (3330 to 3275 cm^{-1}), confirming the decrease in the number of free O−H groups. A single peak at 1642 cm^{-1} in PVA is due to the deformation vibration of the absorbed water molecules.[61] In the case of NBC (M-1), a peak at 1642 cm^{-1} is due to water molecules in the amorphous region (H−O−H bending peak of absorbed water molecules) reappearing in the NBC-incorporated PVA membrane; its intensity increased with an increase in the NBC content. This signifies good compatibility between PVA and NBC, leading to good membranes for packaging applications.

Figure 6B shows the spectra of formaldehyde and its cross-linked NBC-incorporated PVA membranes. In the formaldehyde spectrum, a broad band appeared at 3336 cm^{-1} due to O−H stretching of the moisture content and there was peak at 1642 cm^{-1} for C═O of the aldehyde group.[67] However, the characteristic C═O peak that appeared at 1642 cm^{-1} in the formaldehyde spectrum was not observed in the PVA-10 mass % NBC composite membrane. In addition to this, a new small band appeared at 1159 cm^{-1} and was assigned to C−O−C which is due to the presence of an acetal linkage and also C−O−C bridges of the NBC.[41,54] Further, peaks at 1050 and 1109 cm^{-1} corresponding to C−O−C and C−O stretching vibrations were much broader in the spectrum of PVA-10 mass % NBC membrane compared to those for M-PVA; this suggested a reaction between the −CHO group of the formaldehyde and −OH groups of PVA and NBC.[41] FTIR spectra of stretching, bending, and ring vibrations of −OH, C═O, C−O−C, and H−O−H are given in the Supporting Information.

Thermogravimetric Analysis (TGA). Figure 7 shows the thermogravimetric analysis (TGA) and differential thermogravimetric (DTG) curves for PVA, NBC, and NBC-incorporated PVA membranes. The weight loss was measured in the temperature range of 30−600 °C. All samples showed an initial weight loss at around 100 °C caused by water evaporation from the samples. The NBC peak consists of one decomposition peak starting at 200 °C. Consequently, DTG curves display the degradation peaks at the maximum temperature of 234 °C due to the breakdown of the amorphous part of NBC. Further, the DTG curve displayed no degradation peak, possibly due to the presence of NBC particles.[68] However, the TGA curves for NBC-incorporated PVA membranes showed decomposition trends similar to that of PVA. This was expected due to a greater percentage of PVA in the developed membranes. The DTG curves for NBC-incorporated PVA membranes showed that the weight loss shifted to a higher temperature, 354 °C for pristine PVA[69] to 375 °C for 10 mass % of NBC in the PVA matrix. This was due to the intermolecular interactions and hydrogen bonds between NBC and PVA. A further increase in NBC content DTG curves caused a slight shift to a lower temperature of 371 °C for 15 mass % NBC and 364 °C for 20 mass % NBC. This may be due to formation a highly disordered and agglomerated position with a platelike structure of NBC in the PVA matrix, which was also supported by FESEM images.[68]

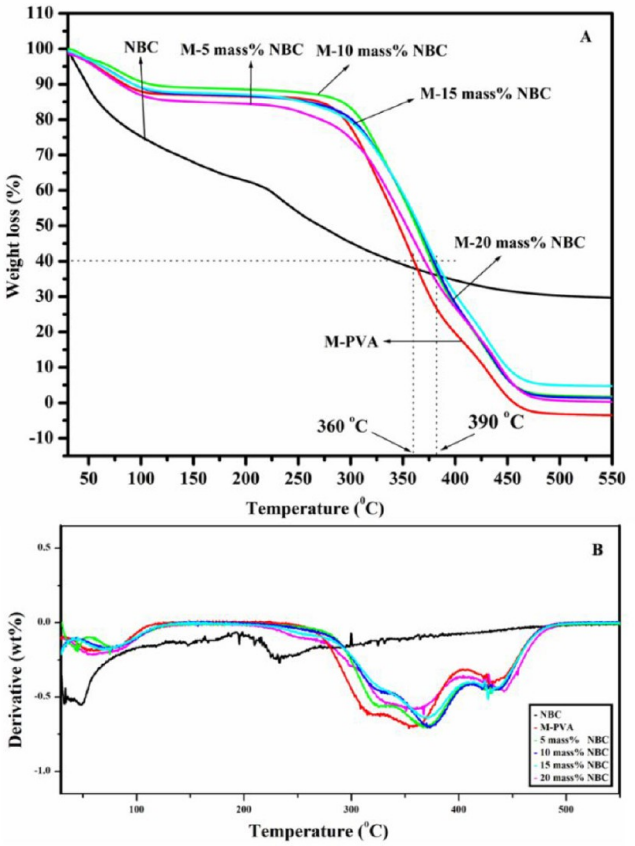

Figure 7. (A) Thermogravimetric and (B) DTG analysis of M-PVA, NBC, M-5 mass % NBC, M-10 mass % NBC; M-15 mass % NBC, and M-20 mass % NBC.

Field Emission Scanning Electron Microscopy (FESEM). Morphological studies of the membranes were performed using FESEM, which gives information about the presence of voids, homogeneity, aggregates, and the distribution of NBC in the PVA matrix. Figure 8 shows the FESEM images of PVA, NBC, and NBC-incorporated PVA membranes. Figure 8A exhibits an image of pure PVA, having a smooth surface.[70] Figure 8B exhibits an image of NBC, with a sponge, sheetlike structure and honeycomb-like pores. The surface images of NBC-incorporated PVA membranes (Figure 8C,D) exhibited a highly ordered and smooth disagglomeration position of NBC due to the formation of hydrogen bonds, interactions, and adhesion between PVA and NBC.[71−74]

On further increase in the mass percent of NBC (Figure 8E,F), images exhibited a highly disordered and agglomeration position with a platelike structure.[72,73] The WAXD, TGA, and DTG support this evidence.

Mechanical Strength Analysis. The practicality of a packaging membrane is defined by mechanical strength, which is comparably higher in the case of nonbiodegradable polymer membranes than in biodegradable polymeric membranes. The mechanical strength of the developed membranes generally depends on the chemical microstructure and the nature of the film-forming materials.[62] Table 1 show the analyzed values of percent elongation at break and the tensile strength of the developed membranes. From the results shown in Table 1, it was observed that cross-linking of the developed membrane by formaldehyde had an impact on the values of percent elongation at the break and tensile strength.

https://doi.org/10.1021/acsomega.2c04336
ACS Omega 2022, 7, 43559−43573

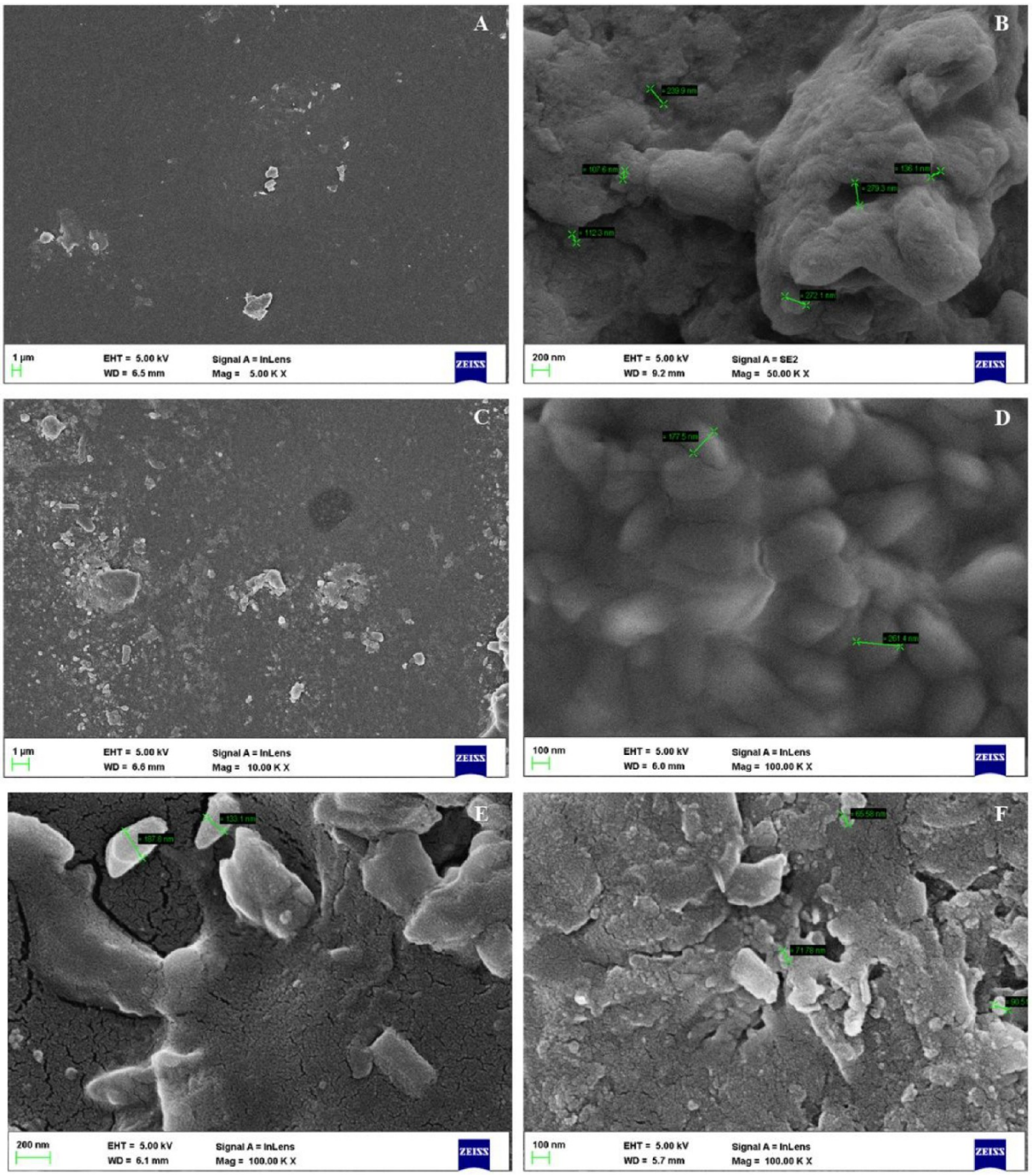

Figure 8. FESEM micrographs of M-PVA (A), NBC (B), M-5 mass % NBC (C), M-10 mass % NBC (D), M-15 mass % NBC (E), and M-20 mass % NBC (F).

Table 1. Ultimate Tensile Strength and Percent Elongation at Break Values of the Developed Membrane

	non-cross-linked membrane		cross-linked membrane	
membrane	TS (MPa)	EAB (%)	TS (MPa)	EAB (%)
M-PVA	12.59	151.89	48.32	191.13
M-5 mass % NBC	12.73	176.81	51.76	219.56
M-10 mass % NBC	12.93	196.64	53.33	235.30
M-15 mass % NBC	12.40	166.14	45.53	215.05
M-20 mass % NBC	12.39	151.53	43.40	210.40

The PVA membrane exhibited a tensile strength of 12.59 MPa.[75] Further, with the addition of NBC into PVA up to 10 mass %, the tensile strength increased slightly from 12.73 to 12.93 MPa, and the percent elongation at break increased from 151.89% to 196.64%. This behavior of the developed membrane may be due to a strong interfacial interaction, good dispersibility, and excellent adhesion between NBC and PVA in the membrane.[76−79] The increase in tensile strength and percent elongation at break of the developed membrane is due to the availability of hydroxyl functionalities in large numbers on the surface of NBC, resulting in the formation of hydrogen bonds by interacting with the PVA membrane. A

https://doi.org/10.1021/acsomega.2c04336
ACS Omega 2022, 7, 43559−43573

slightly decreased tensile strength and percent elongation at break was observed beyond the addition of 10 mass % NBC; this may be attributed to the agglomeration of NBC, resulting in a poor distribution of NBC across the PVA membrane. NBC hinders its homogeneous dispersion in the PVA matrix and weakens the hydrogen bond interaction between NBC and PVA.[80] Figure 9 shows the tensile strength and percent

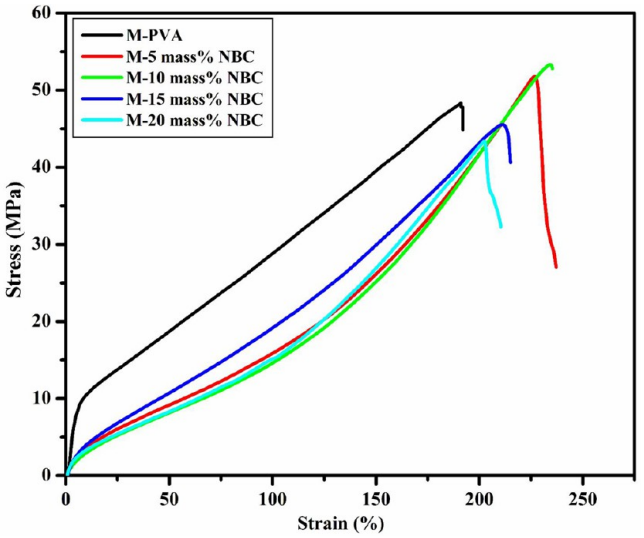

Figure 9. Tensile stress−strain curves of M-PVA, M-5 mass % NBC, M-10 mass % NBC, M-15 mass % NBC, and M-20 mass % NBC.

elongation at break values of PVA and NBC-incorporated cross-linked membranes. As the NBC content increased from 5% to 10% in PVA, tensile strength and percent elongation values at break increased from 48.32 to 53.33 MPa and from 191.13% to 235.30%, respectively, due to hydrogen bonding and high crystallinity. However, from the membranes M-15 mass % NBC to M-20 mass% NBC, the tensile strength and percent elongation at break values slightly decreased with an increase in NBC content in the M-PVA matrix, which is due to a disturbance in the arrangement of PVA chains, which makes the membranes more amorphous.[76,81] When the NBC content was above 10 mass % in the PVA matrix, intermolecular interactions between the NBC molecules increased by replacing the interactions between NBC and PVA molecules.[59] From Figure 9, M-10 mass % NBC exhibited the highest tensile strength and percent elongation at break.

Water Vapor Transmission Rate (WVTR). WVTR is the steady-state rate of permeability of water vapors through a membrane at a specified temperature for a given time. A membrane that resists the permeation of water vapors from an external source to the inside is said to be suitable for food packaging applications. Water activity is the ratio of the vapor pressure of water in the substrate to that of pure water at the same temperature. It is the main reason for the growth of microorganisms, and hence a low water activity prevents the growth of microorganisms.[77] Membranes with a low WVTR will allow less water permeation from an external source to the inside, resulting in a low water activity and protecting the food from spoilage.[58]

Laxmeshwar et al.[59] reported that the WVTR decreases as the cellulose concentration increases. This change is attributed to decreased hydrophilicity due to increased cellulosic content. Therefore, hydrogen-bonding interactions play an important role in the WVTR. The water vapor transmission rate decreases with an increase in the NBC content. This is mainly due to an increase in hydrogen bonds between NBC and PVA as the NBC concentration increases, which reduces the number of free O−H groups. The FTIR spectra also confirm this, wherein the intensity of the broad band at 3330 cm^{-1} decreases as the concentration of NBC increases. The compact bonding between PVA and NBC increases the tortuosity, allows the films to behave as a barrier to the permeation of water vapors through them, and reduces the WVTR at a higher concentration of NBC.

Table 2 demonstrates the WVTR in g/(m^2 h) of all the developed membranes. M-PVA has a WVTR of 15.49 g/(m^2 h), as the free O−H groups allow more permeation of water vapor through the membrane. In contrast, the PVA/NBC membrane with an NBC concentration of 20% has the lowest WVTR of 8.86 g/(m^2 h) due to fewer O−H groups, which allow a resistance to permeation of water vapors.

Table 2. Barrier Properties of the Developed Composite Membranes

membrane designation	water vapor transmission rate (g/(m^2 h))	degree of swelling (%)	moisture retention capability (%)	membrane solubility (%)
M-PVA	15.49	53	88.88	9.32
M-5 mass % NBC	12.57	41	93.12	9.27
M-10 mass % NBC	11.40	36	93.57	9.26
M-15 mass % NBC	9.98	24	93.69	9.13
M-20 mass % NBC	8.67	18	94.18	9.09

Moisture Retention Capability (MRC). Loss of water vapors from the membranes is known as the moisture retention capability of the membranes. The taste, texture, and quality of the packed food within the packaging material are maintained based on the material's ability for moisture movement.[57] A variety of available foods require a different moisture level to be maintained to preserve the food for a longer period.

The hydrophilic nature of the membranes contributes to the good moisture retention capability. The free O−H groups are responsible for holding the water inside the membranes. Table 2 depicts the MRC of all the developed membranes. The

Table 3. Zone of Clearance of Various Membranes against Four Different Pathogens

SL No.	pathogen	membrane designation	zone of clearance (mm)
1	*E. coli*	M-10 mass % NBC	35
		M-15 mass % NBC	45
		M-20 mass % NBC	50
2	*S. aureus*	M-10 mass % NBC	40
		M-15 mass % NBC	42
		M-20 mass % NBC	50
3	*B. cereus*	M-10 mass % NBC	35
		M-15 mass % NBC	38
		M-20 mass % NBC	40
4	*M. luteus*	M-10 mass % NBC	30
		M-15 mass % NBC	40
		M-20 mass % NBC	50

https://doi.org/10.1021/acsomega.2c04336
ACS Omega 2022, 7, 43559−43573

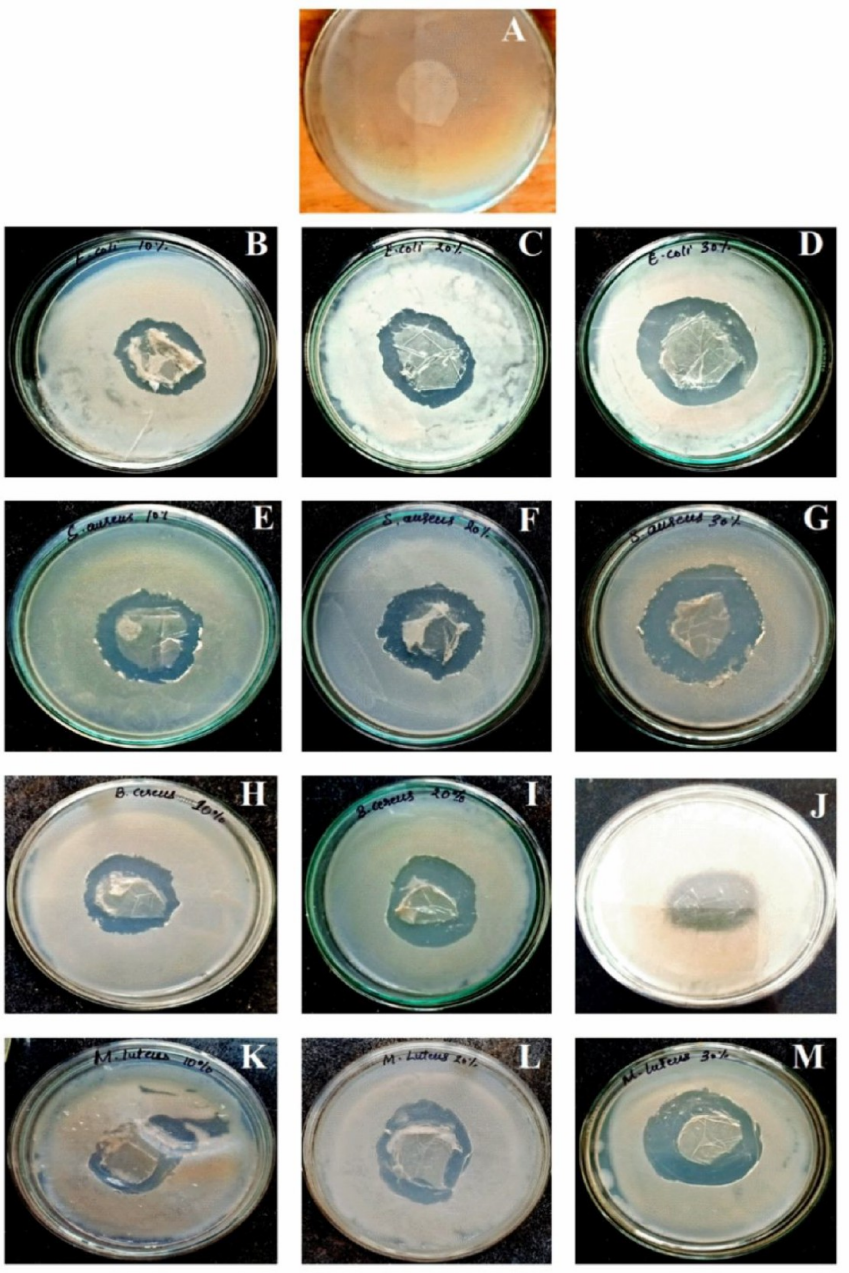

Figure 10. Picture depicting antimicrobial activity against pathogens by producing a zone of clearance: (A) control; for *E. coli* (B) M-10 mass % NBC, (C) M-15 mass % NBC, and (D) M-20 mass % NBC; for *S. aureus* (E) M-10 mass % NBC, (F) M-15 mass % NBC, and (G) M-20 mass % NBC; for *B. cereus* (H) M-10 mass % NBC, (I) M-15 mass % NBC, and (J) M-20 mass % NBC; for *M. luteus* (K) M-10 mass % NBC, (L) M-15 mass % NBC, and (M) M-20 mass% NBC.

results provide an increasing trend in MRC percent with an increase in the NBC content. As was previously discussed, with an increase in the NBC content, the availability of free O−H groups decreases. These free groups are responsible for maintaining the hydration level by penetrating the structure of NBC. All membranes exhibited good moisture retention capability in the range of 78−95%, which is the standard moisture retention capability range provided by ITC Limited, India. The pristine PVA membrane (M-PVA) resulted in the lowest MRC, whereas PVA/NBC membranes with various NBC contents had a high MRC, with no significant difference.

Swelling Measurement (SM). Table 2 depicts the swelling studies of the developed membranes that play an important role in defining the practical application of the membranes. Various factors that affect swelling are the type of material, network density, pH, temperature, hydration capacity, and ionic strength of the membranes.[82,83] M-PVA, being a hydrophilic material, results in 53% swelling due to the absorption of water molecules. PVA/NBC composite membranes show relatively low swelling compared to M-PVA due to incorporation of various mass percents of NBC. The degree of swelling varies from 41%, the highest for the PVA/NBC membranes, to 18% as the lowest. Swelling of the PVA/NBC membranes (M-5 mass % NBC to M-20 mass % NBC) decreases significantly as the mass percent of NBC increases.

https://doi.org/10.1021/acsomega.2c04336
ACS Omega 2022, 7, 43559−43573

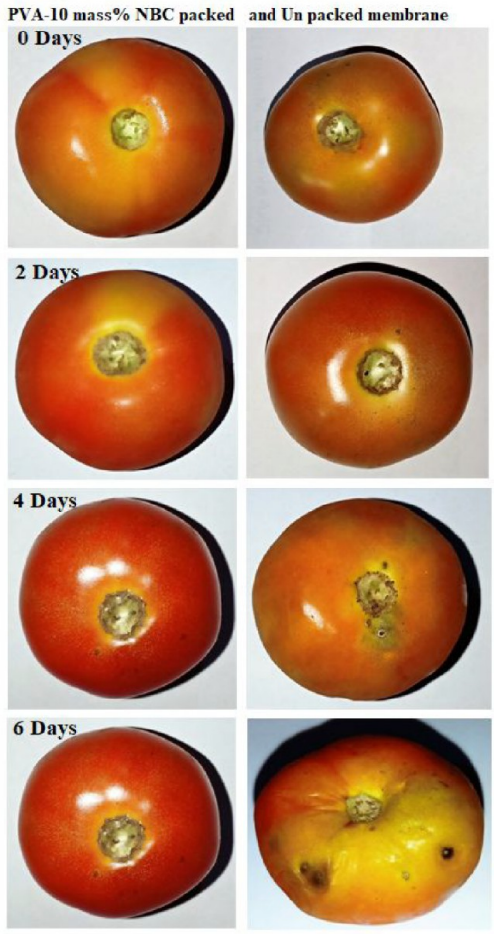

Figure 11. Images of changes in the external appearance of membrane-packed and unpacked tomatoes for various storage times.

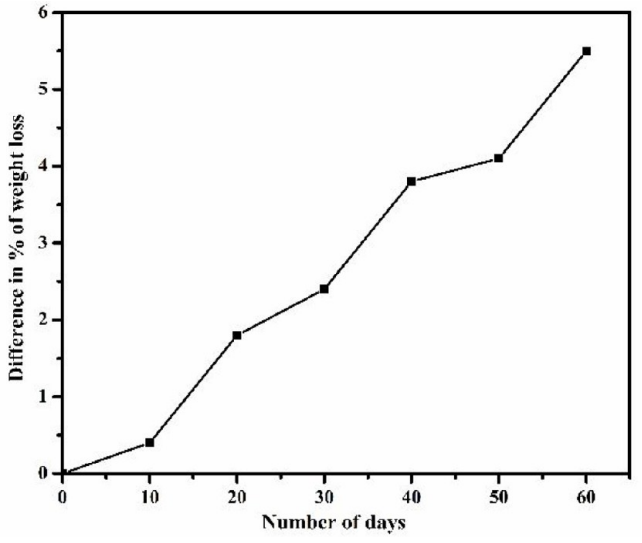

Figure 12. Degradation of M-10 mass % NBC membrane in the soil.

This is due to the reinforcing NBC material that reduces the hydration and flexibility of the films.

Membrane Solubility (MS). A necessary characteristic of a membrane for the application of food packaging is the insolubility of the membranes. This characteristic imparts improved product quality and extended shelf life due to moisture control, which retards microbial growth and prevents the rotting of fruits and vegetables.[84] Table 2 indicates the percentage of membrane solubility, and all of the values show little difference. The results illustrate that M-PVA has the highest solubility and that the solubility of the composite membranes decreases as NBC is incorporated into PVA. Cross-linked membranes have reduced membrane solubility to a greater extent. Membrane solubility shows an inversely proportional trend to the NBC mass percent in the PVA membrane. Therefore, M-20 mass % NBC shows the least membrane solubility.

Antibacterial Activity Measurements. An important criterion for the characterization of food packaging application is antibacterial activity. This was determined by the zone of clearance of the developed membranes with various mass percents of NBC against *E. coli*, *S. aureus*, *B. cereus*, and *M. luteus*. The zone of clearance values are given in Table 3.

Figure 10 shows that the PVA(M) membrane showed no antibacterial activity, which confirms that the antibacterial activity of membranes (M-10 mass % NBC to M-20 mass % NBC) was due to the content of NBC in the membrane matrix. An increase in the mass % of NBC increases the antibacterial activity of the membranes. The membrane M-15 mass % NBC with maximum NBC content resulted in the highest zone of clearance for all four bacteria. NBC exhibits antimicrobial properties due to a physical interaction between NBC and the outer membrane of bacteria, thereby developing physical stress on the phospholipid bilayer membrane of the bacteria. This contact-mediated mechanism destroys the phospholipid bilayer membrane, thereby causing the loss of membrane integrity and morphological damage to bacterial cells, which results in the inactivation of the bacteria that come in contact with the NBC-incorporated PVA membrane.[36] Membranes showed relatively less antibacterial activity for *S. aureus*, *M. luteus*, and *B. cereus* in comparison to *E. coli*. This is due to the fact that Gram-positive bacteria (*S. aureus*, *M. luteus*, and *B. cereus*) have thicker cell walls than Gram-negative bacteria, which has a thin peptidoglycan layer that makes penetration of NBC into *E. coli* trouble-free and hence inhibits the bacterial growth to a greater extent.[59]

Packaging Ability. Tomato, botanically called *Solanum lycopersicum*, always requires a refrigerator for preservation. The primary pathogen that causes spoilage of tomatoes is the fungus *Colletotrichum coccoides*, and the disease is known as anthracnose. The development of dark circular patches further increases over time. As shown in Figure 11, an unpacked tomato is attacked by anthracnose, whereas the tomato packed with the optimized membrane exhibits no disease. This was due to the antimicrobial property of the membrane. Hence, the tomato was prevented from microbial spoilage for more than 10 days.

Biodegradability Test. A biodegradability test was conducted to understand the ability of the developed membrane to be degraded by microorganisms in the soil. Biodegradation of the membrane M-10 mass % NBC is shown in Figure 12. From the figure, it is clear that an increase in incubation days increases the percent of weight loss proportionally, thereby revealing the degradation ability of the membrane. PVA(M) and cellulose present in the membrane act as a carbon source for microorganisms. NBC-incorporated PVA membranes degrade by the action of active microorganisms in the soil.

https://doi.org/10.1021/acsomega.2c04336
ACS Omega 2022, 7, 43559−43573

The biodegradable ability of the developed membranes depends on the amorphous and crystalline parts of the polymer chain. The amorphous region of the NBC-incorporated membrane degrades first by the action of microorganisms. Fifty-five species of microorganisms, including bacteria, fungi, and yeast, degrade PVA.[85,86] The incorporation of NBC in PVA enhanced the biodegradation process of the PVA membrane.[87] Biodegradation of the developed membrane was slow during the initial 10 days and was up to 0.5% weight loss due to the antibacterial activity of NBC in the membrane. After 10 days of incubation in the soil, the weight loss was enhanced from 0.5% to 6% due to the action of different microorganisms such as bacteria, fungi, and yeast present in the soil at the amorphous region of the membrane. Initially, microbial flora produce cellulose enzymes for biodegradation of NBC, thereby changing the physical and chemical properties of the membrane by disturbing the compatibility of NBC and PVA.[88] After the loss of compatibility between NBC and PVA, NBC completely degrades to CO_2, methane, water, and biomass.[88] Later, PVA degradation will be initiated by PVA-degrading enzymes such as poly(vinyl alcohol) dehydrogenase,[89] laccase, and PVA oxidase. Different mechanisms of biodegradation of PVA have been reported.[90] In one mechanism, PVA degradation leads to the formation of β-hydroxyketone groups, later cleaved by hydrolase to form carboxyl- and methyl-terminated degradation products.

CONCLUSIONS

In this research work, an NBC-producing bacterial strain was isolated, screened, and molecularly characterized as *Bacillus subtilis* strain LRP1. Further, the produced NBC with different mass percents was incorporated with PVA to develop PVA-NBC composite membranes using a solution casting technique. A zetasizer using the DLS technique revealed that the hydrodynamic size and ζ potential of bacterial cellulose were 108 nm and −53.6 mV, respectively. The crystallite size of the BC was 113 nm which indicates bacterial cellulose as NBC. A shift of FTIR peak from 3330 to 3275 cm^{-1} was due to hydrogen bonding between PVA and NBC. An FTIR peak for C═O of an aldehyde group at 1642 cm^{-1} did not appear in the PVA-10 mass % NBC membrane, indicating that the developed membranes are free from aldehyde. The thermal stability of the NBC-incorporated PVA membranes was enhanced by 30 °C compared to the PVA membrane. The formaldehyde cross-linked M-10 mass % NBC membrane exhibited a 53.33 MPa tensile strength with a percent elongation at break of 235.30, suggesting that the membrane is suitable for packaging applications. The M-10 mass % NBC membrane showed a water vapor transmission rate of 11.40 g/(m^2 h), a degree of swelling of 36%, a moisture retention capability of 93.57%, and a membrane solubility of 9.26%. The zone of clearance against pathogens such as *E. coli*, *S. aureus*, *B. cereus*, and *M. luteus* increases with an increase in mass percent of NBC. Tomatoes were packed with an M-10 mass % NBC membrane, which prevented the fruit from microbial attachment for up to 10 days and underwent biodegradation within 1 year. Hence, the M-10 mass % NBC membrane can be used for food packaging applications.

ASSOCIATED CONTENT

Supporting Information

The Supporting Information is available free of charge at https://pubs.acs.org/doi/10.1021/acsomega.2c04336.

Supplementary table for FTIR spectra of PVA, NBC, and NBC-incorporated PVA nanocomposite membranes (PDF)

AUTHOR INFORMATION

Corresponding Author

Ashok M. Sajjan − *Department of Chemistry, KLE Technological University, Hubballi 580031, India; Center of Excellence in Material Science, KLE Technological University, Hubballi 580031, India;* orcid.org/0000-0003-1251-8803; Phone: +91-944-8801139; Email: ashokmsajjan@gmail.com; Fax: +91-836-2374985

Authors

Manu L. Naik − *Department of Chemistry, KLE Technological University, Hubballi 580031, India*

Ashwini M − *AICRP on EAAI (Bioconversion Technology), University of Agricultural Sciences, Dharwad 580005, India*

Sharanappa Achappa − *Department of Biotechnology, KLE Technological University, Hubballi 580031, India*

T. M. Yunus Khan − *Department of Mechanical Engineering, College of Engineering, King Khalid University, Abha 61421, Saudi Arabia*

Nagaraj R. Banapurmath − *Center of Excellence in Material Science, KLE Technological University, Hubballi 580031, India*

Prakash B. Kalahal − *Department of Chemistry, KLE Technological University, Hubballi 580031, India*

Narasimha H. Ayachit − *Center of Excellence in Material Science, KLE Technological University, Hubballi 580031, India*

Complete contact information is available at: https://pubs.acs.org/10.1021/acsomega.2c04336

Author Contributions

A.M.S., A.M, S.A., M.L.N.: conceptualization, methodology, writing-original draft preparation. A.M.S., A.M., S.A., N.R.B., P.B.K., T.M.Y.K., N.H.A.: conceptualization, writing-review and editing, formal analysis. A.M.S., A.M.: supervision. A.M.S., A.M., S.A., N.R.B.: investigation. A.M.S., A.M., S.A.: project administration.

Notes

The authors declare no competing financial interest.

ACKNOWLEDGMENTS

A.M.S. gratefully acknowledges financial support from the Vision Group on Science and Technology, Karnataka, India (no. K-FIST (L2)/2016-17/GRD-540/2017-18/103/130). A.M. and A.M.S. wish to acknowledge the University of Agricultural Sciences, Dharwad, for extending financial support (DR-SRP/SCP/TSP/T-4/4.1/15/2019-20/4931-B).

REFERENCES

(1) Ilyas, M.; Ahmad, W.; Khan, H.; Yousaf, S.; Khan, K.; Nazir, S. Plastic waste as a significant threat to environment−a systematic literature review. *Rev. environ. health.* **2018**, *33* (4), 383−406.

(2) Chen, Y.; Awasthi, A. K.; Wei, F.; Tan, Q.; Li, J. Single-use plastics: Production, usage, disposal, and adverse impacts. *Sci. of the total. environ.* **2021**, *752*, 141772.

(3) Ncube, L. K.; Ude, A. U.; Ogunmuyiwa, E. N.; Zulkifli, R.; Beas, I. N. An overview of plastic waste generation and management in food packaging industries. *Recycling* **2021**, *6* (1), 12.

(4) Campos, C. A.; Gerschenson, L. N.; Flores, S. K. Development of edible films and coatings with antimicrobial activity. *Food and bioprocess technology* **2011**, 849−875.
(5) Rudnik, E.*Handbook of Biopolymers and Biodegradable Plastics*; Elsevier: 2008
(6) Conte, A.; Angiolillo, L.; Mastromatteo, M.; Del Nobile, M. A. Technological Options of Packaging to Control Food Quality. *Food Quality* **2013**, 357−379.
(7) Sorrentino, A.; Gorrasi, G.; Vittoria, V. Potential perspectives of bio-nanocomposites for food packaging applications. *Trends in food scie & technology* **2007**, *18* (2), 84−95.
(8) Bianco, A.; Di Federico, E.; Cacciotti, I. Electrospun poly (ε-caprolactone)-based composites using synthesized β-tricalcium phosphate. *Polym. for Adv. Technol.* **2011**, *22* (12), 1832−41.
(9) Kulkarni, A. S.; Sajjan, A. M.; Khan, T. Y.; Badruddin, I. A.; Kamangar, S.; Banapurmath, N. R.; Ayachit, N. H.; Ashwini, M.; Sharanappa, A. Development and Characterization of Biocompatible Membranes from Natural Chitosan and Gelatin for Pervaporative Separation of Water−Isopropanol Mixture. *Polym.* **2021**, *13* (17), 2868.
(10) Sajjan, A. M.; Kariduraganavar, M. Y. Development of novel membranes for PV separation of water−isopropanol mixtures using poly (vinyl alcohol) and gelatin. *J. of memb sci* **2013**, *438*, 8−17.
(11) Yat, S. C.; Berger, A.; Shonnard, D. R. Kinetic characterization for dilute sulfuric acid hydrolysis of timber varieties and switchgrass. *Bioresourctechnol* **2008**, *99* (9), 3855−3863.
(12) Kumar, P.; Barrett, D. M.; Delwiche, M. J.; Stroeve, P. Methods for pretreatment of lignocellulosic biomass for efficient hydrolysis and biofuel production. *Ind. Eng. Chem. Res.* **2009**, *48* (8), 3713−3729.
(13) Sánchez, C. Lignocellulosic residues: biodegradation and bioconversion by fungi. *Biotechnol Adv.* **2009**, *27* (2), 185−94.
(14) Iqbal, H. M.; Kyazze, G.; Keshavarz, T. Advances in the valorization of lignocellulosic materials by biotechnology: an overview. *Bio Resource* **2013**, *8* (2), 3157−3176.
(15) Tajeddin, B. Cellulose-based polymers for packaging applications. *Ligno Polym. Comptes* **2014**, 477−98.
(16) Jamróz, E.; Kulawik, P.; Kopel, P. The effect of nanofillers on the functional properties of biopolymer-based films: A review. *Polym.* **2019**, *11* (4), 675.
(17) Wyrwa, J.; Barska, A. Innovations in the food packaging market: Active packaging. *Eur. Food Res. Technol.* **2017**, *243* (10), 1681−92.
(18) Marsh, K.; Bugusu, B. Food packaging roles, materials, and environmental issues. *J. of food sci* **2007**, *72* (3), R39−R55.
(19) Han, J.-W.; Ruiz-Garcia, L.; Qian, J.-P.; Yang, X.-T. Food packaging: A comprehensive review and future trends. *Compre Rev. in Food Sci. and Food Safety* **2018**, *17* (4), 860−877.
(20) Zhong, Y.; Godwin, P.; Jin, Y.; Xiao, H. Biodegradable polymers and green-based antimicrobial packaging materials: A mini-review. *Advanced Industrial and Engineering Polymer Research* **2020**, *3* (1), 27−35.
(21) Adlhart, C.; Verran, J.; Azevedo, N. F.; Olmez, H.; Keinänen-Toivola, M. M.; Gouveia, I.; Melo, L. F.; Crijns, F. Surface modifications for antimicrobial effects in the healthcare setting: A critical overview. *J. of Hosp Infect* **2018**, *99* (3), 239−249.
(22) Cloutier, M.; Mantovani, D.; Rosei, F. Antibacterial coatings: challenges, perspectives, and opportunities. *Trends Biotechnol.* **2015**, *33* (11), 637−52.
(23) Perreault, F.; De Faria, A. F.; Nejati, S.; Elimelech, M. Antimicrobial properties of graphene oxide nanosheets: why size matters. *ACS Nano* **2015**, *9* (7), 7226−7236.
(24) Liu, C.; Lee, J.; Small, C.; Ma, J.; Elimelech, M. Comparison of organic fouling resistance of thin-film composite membranes modified by hydrophilic silica nanoparticles and zwitterionic polymer brushes. *J. Membr. Sci.* **2017**, *544*, 135−42.
(25) Yang, W. J.; Neoh, K. G.; Kang, E. T.; Teo, S. L.; Rittschof, D. Polymer brush coatings for combating marine biofouling. *ProgrsPolym. Sci.* **2014**, *39* (5), 1017−1042.
(26) Grishkewich, N.; Mohammed, N.; Tang, J.; Tam, K. C. Recent advances in the application of cellulose nanocrystals. *Curr. Opin. Colloid Interface Sci.* **2017**, *29*, 32−45.
(27) Trache, D.; Hussin, M. H.; Haafiz, M. M.; Thakur, V. K. Recent progress in cellulose nanocrystals: source and production. *Nanoscale* **2017**, *9* (5), 1763−1786.
(28) Yoksan, R.; Chirachanchai, S. Silver nanoparticle-loaded chitosan−starch based films: Fabrication and evaluation of tensile, barrier and antimicrobial properties. *Mater. Sci. and Engg: C* **2010**, *30* (6), 891−7.
(29) Boschetto, D. L.; Lerin, L.; Cansian, R.; Pergher, S. B.; Di Luccio, M. Preparation and antimicrobial activity of polyethylene composite films with silver exchanged zeolite-Y. *Chem. Engg J.* **2012**, *204-206*, 210−216.
(30) Hoseinnejad, M.; Jafari, S. M.; Katouzian, I. Inorganic and metal nanoparticles and their antimicrobial activity in food packaging applications. *Critirevi in microbio* **2018**, *44* (2), 161−181.
(31) Sabharwal, P. K.; Chattopadhyay, S.; Singh, H. Preparation and characterization of antimicrobial, biodegradable, triclosan-incorporated polyhydroxybutyrate-co-valerate films for packaging applications. *J. Applid Polym. Sci.* **2018**, *135* (44), 46862.
(32) Muñoz-Bonilla, A.; Echeverria, C.; Sonseca, Á.; Arrieta, M. P.; Fernández-García, M. Bio-based polymers with antimicrobial properties towards sustainable development. *Mater.* **2019**, *12* (4), 641.
(33) Seabra, A. B.; Bernardes, J. S.; Fávaro, W. J.; Paula, A. J.; Durán, N. Cellulose nanocrystals as carriers in medicine and their toxicities: A review. *Carbohydpolym* **2018**, *181*, 514−527.
(34) El-Samahy, M. A.; Mohamed, S. A.; Rehim, M. H.; Mohram, M. E. Synthesis of hybrid paper sheets with enhanced air barrier and antimicrobial properties for food packaging. *CarbohydPolym.* **2017**, *168*, 212−219.
(35) Tyagi, P.; Mathew, R.; Opperman, C.; Jameel, H.; Gonzalez, R.; Lucia, L.; Hubbe, M.; Pal, L. High-strength antibacterial chitosan−cellulose nanocrystal composite tissue paper. *Langmuir* **2019**, *35* (1), 104−12.
(36) Noronha, V. T.; Camargos, C. H.; Jackson, J. C.; Souza Filho, A. G.; Paula, A. J.; Rezende, C. A.; Faria, A. F. Physical membrane-stress-mediated antimicrobial properties of cellulose nanocrystals. *ACS Sust Chem. Engg* **2021**, *9* (8), 3203−3212.
(37) Madera-Santana, T. J.; Freile-Pelegrín, Y.; Azamar-Barrios, J. A. Physicochemical and morphological properties of plasticized poly (vinyl alcohol)−agar biodegradable films. *Inter j biology macromol* **2014**, *69*, 176−184.
(38) Shagholani, H.; Ghoreishi, S. M.; Mousazadeh, M. Improvement of interaction between PVA and chitosan via magnetite nanoparticles for drug delivery application. *Inter j biologmacromol* **2015**, *78*, 130−136.
(39) Gutha, Y.; Pathak, J. L.; Zhang, W.; Zhang, Y.; Jiao, X. Antibacterial and wound healing properties of chitosan/poly (vinyl alcohol)/zinc oxide beads (CS/PVA/ZnO). *Inter j biologmacromol* **2017**, *103*, 234−241.
(40) Jiang, X.; Li, H.; Luo, Y.; Zhao, Y.; Hou, L. Studies of the plasticizing effect of different hydrophilic inorganic salts on starch/poly (vinyl alcohol) films. *Inter J. BiologMacromol.* **2016**, *82*, 223−30.
(41) Cazón, P.; Vázquez, M. Bacterial cellulose as a biodegradable food packaging material: A review. *Food Hydrocolloids* **2021**, *113*, 106530.
(42) Ju, S.; Zhang, F.; Duan, J.; Jiang, J.; et al. Characterization of bacterial cellulose composite films incorporated with bulk chitosan and chitosan nanoparticles: A comparative study. *Carbohyd. polym.* **2020**, *237*, 116167.
(43) Mihaela Jipa, I.; Dobre, L.; Stroescu, M.; Stoica-Guzun, A.; Jinga, S.; Dobre, T. Preparation and characterization of bacterial cellulose-poly(vinyl alcohol) films with antimicrobial properties. *Mater. Lett.* **2012**, *66*, 125−127.
(44) He, H.; Cai, R.; Wang, Y.; Tao, G.; Guo, P.; Zuo, H.; Chen, L.; Liu, X.; Zhao, P.; Xia, Q. Preparation and characterization of silk sericin/PVA blend film with silver nanoparticles for potential antimicrobial application. *Inter j biologmacromol* **2017**, *104*, 457−64.

https://doi.org/10.1021/acsomega.2c04336
ACS Omega 2022, 7, 43559−43573

(45) Bano, I.; Ghauri, M. A.; Yasin, T.; Huang, Q.; Palaparthi, A. D. Characterization and potential applications of gamma irradiated chitosan and its blends with poly (vinyl alcohol). *Int. J. BiolMacromol.* **2014**, *65*, 81−88.
(46) Popescu, M. C.; Dogaru, B. I.; Goanta, M.; Timpu, D. Structural and morphological evaluation of CNC reinforced PVA/Starch biodegradable films. *Int. J. BiolMacromol.* **2018**, *116*, 385−393.
(47) Wang, J.; Gao, C.; Zhang, Y.; Wan, Y. Preparation and in vitro characterization of BC/PVA hydrogel composite for its potential use as artificial cornea biomaterial. *Mater. Sci. and Engg: C* **2010**, *30* (1), 214−8.
(48) RamezaniKakroodi, A.; Cheng, S.; Sain, M.; Asiri, A. Mechanical, thermal, and morphological properties of nanocomposites based on polyvinyl alcohol and cellulose nanofiber from Aloe vera rind. *J. Nanomater.* **2014**, *2014*, 1−7.
(49) Millon, L. E.; Wan, W. K. The polyvinyl alcohol-bacterial cellulose system as a new nanocomposite for biomedical applications. *J. Biomed. Mater. Res.* **2006**, *79B* (2), 245−253.
(50) Abba, M.; Abdullahi, M.; Md Nor, M. H.; Chong, C. S.; Ibrahim, Z. Isolation and characterisation of locally isolated Gluconacetobacterxylinus BCZM sp. with nanocellulose producing potentials. *IET Nanobiotechnol* **2018**, *12* (1), 52−56.
(51) Rangaswamy, B. E.; Vanitha, K. P.; Hungund, B.S. Microbial cellulose production from bacteria isolated from rotten fruit. *Inter j polym sci* **2015**, *2015*, 1−8.
(52) Thongwai, N.; Futui, W.; Ladpala, N.; Sirichai, B.; Weechan, A.; Kanklai, J.; Rungsirivanich, P. Characterization of Bacterial Cellulose Produced by Komagataeibactermaltaceti P285 Isolated from Contaminated Honey Wine. *Microorgsm* **2022**, *10* (3), 528.
(53) Gopu, G.; Govindan, S. Production of bacterial cellulose from Komagataeibactersaccharivorans strain BC1 isolated from rotten green grapes. *Prep Biochem and Biotechnol* **2018**, *48* (9), 842−52.
(54) Qiu, K.; Netravali, A. N. Bacterial cellulose-based membrane-like biodegradable composites using cross-linked and noncross-linked polyvinyl alcohol. *J. Mater. Sci.* **2012**, *47* (16), 6066−6075.
(55) Frone, A. N.; Panaitescu, D. M.; Nicolae, C. A.; Gabor, A. R.; Trusca, R.; Casarica, A.; Stanescu, P. O.; Baciu, D. D.; Salageanu, A. Bacterial cellulose sponges obtained with green cross-linkers for tissue engineering. *Mater. Sci. and Engg C* **2020**, *110*, 110740.
(56) Kulkarni, A. S.; Sajjan, A. M.; M, A.; Banapurmath, N. R.; Ayachit, N. H.; Shirnalli, G. G. Novel fabrication of PSSAMA_Na capped silver nanoparticle embedded sodium alginate membranes for pervaporative dehydration of bioethanol. *RSC adv* **2020**, *10* (38), 22645−22655.
(57) Sarwar, M. S.; Niazi, M. B.; Jahan, Z.; Ahmad, T.; Hussain, A. Preparation and characterization of PVA/nanocellulose/Ag nanocomposite films for antimicrobial food packaging. *Carbohydr. Polym.* **2018**, *184*, 453−464.
(58) Aloui, H.; Khwaldia, K.; Hamdi, M.; Fortunati, E.; Kenny, J. M.; Buonocore, G. G.; Lavorgna, M. Synergistic effect of halloysite and cellulose nanocrystals on the functional properties of PVA based nanocomposites. *ACS Sust Chem. &Engg* **2016**, *4* (3), 794−800.
(59) Laxmeshwar, S. S.; Madhu Kumar, D. J.; Viveka, S.; Nagaraja, G. K. Preparation and properties of biodegradable film composites using modified cellulose fibre-reinforced with PVA. *Inter Scholarly Resech Notic* **2012**, *2012*, 1−8.
(60) Sajjan, A. M.; Naik, M. L.; Kulkarni, A. S.; Fazal-E-Habiba Rudgi, U.; M, A.; Shirnalli, G. G.; A, S.; Kalahal, P. B. Preparation and characterization of PVA-Ge/PEG-400 biodegradable plastic blend films for packaging applications. *Chem. Data Collect* **2020**, *26*, 100338.
(61) Stoica-Guzun, A.; Jecu, L.; Gheorghe, A.; Raut, I.; Stroescu, M.; Ghiurea, M.; Danila, M.; Jipa, I.; Fruth, V. Biodegradation of poly (vinyl alcohol) and bacterial cellulose composites by Aspergillus niger. *J. of Polym. and the Environ* **2011**, *19* (1), 69−79.
(62) Pal, S.; Nisi, R.; Stoppa, M.; Licciulli, A. Silver-functionalized bacterial cellulose as antibacterial membrane for wound-healing applications. *ACS omega* **2017**, *2* (7), 3632−9.
(63) Kulkarni, A. S.; Badi, S. M.; Sajjan, A. M.; Banapurmath, N. R.; Karidurаganavar, M. Y.; Shettar, A. S. Preparation and characterization of B2SA grafted hybrid poly (vinyl alcohol) membranes for pervaporation separation of water-isopropanol mixtures. *Chem. Data Collect* **2019**, *22*, 100245.
(64) Kalahal, P. B.; Kulkarni, A. S.; Sajjan, A. M.; Khan, T. Y.; Anjum Badruddin, I.; Kamangar, S.; Banapurmath, N. R.; Ayachit, N. H.; Naik, M. L.; Marakatti, V. S. Fabrication and Physicochemical Study of B2SA-Grafted Poly (vinyl Alcohol)−Graphene Hybrid Membranes for Dehydration of Bioethanol by Pervaporation. *Memb* **2021**, *11* (2), 110.
(65) Pavaloiu, R. D.; Guzun, A. S.; Stroescu, M. Composite membranes of poly(vinyl alcohol)-chitosan-Nano bacterial cellulose or drug controlled release. *Inter J. BiolMacromol.* **2014**, *68*, 117−124.
(66) Mohite, B. V.; Patil, S. V. Physical, structural, mechanical and thermal characterization of bacterial cellulose by G. hansenii NCIM 2529. *Carbohydr. Polym.* **2014**, *106*, 132−141.
(67) AlkhalfMaha, I.; Mirghani, M. E.Detection of formaldehyde in cheese using FTIR spectroscopy. *Inter Res. J.*. **2017**, *24*, 496−500..
(68) Mohd, N. H.; Ismail, N. F.; Zahari, J. I.; Fathilah, W.; Kargarzadeh, H.; Ramli, S.; Ahmad, I.; Yarmo, M. A.; Othaman, R. Effect of aminosilane modification on nanocrystalline cellulose properties. *J. Nanomater.* **2016**, *2016*, 1−8.
(69) Qi, X.; Hu, X.; Wei, W.; Yu, H.; Li, J.; Zhang, J.; Dong, W. Investigation of Salecan/poly (vinyl alcohol) hydrogels prepared by freeze/thaw method. *Carbohydpolym* **2015**, *118*, 60−9.
(70) Zhang, C.; Zhou, M.; Liu, S.; Wang, B.; Mao, Z.; Xu, H.; Zhong, Y.; Zhang, L.; Xu, B.; Sui, X. Copper-loaded nanocellulose sponge as a sustainable catalyst for regioselective hydroboration of alkynes. *Carbohydr. Polym.* **2018**, *191*, 17−24.
(71) Choo, K.; Ching, Y. C.; Chuah, C. H.; Julai, S.; Liou, N. S. Preparation and characterization of polyvinyl alcohol-chitosan composite films reinforced with cellulose nanofiber. *Materials* **2016**, *9* (8), 644.
(72) Jahan, Z.; Niazi, M. B. K.; Gregersen, Ø.W. Mechanical, thermal and swelling properties of cellulose nanocrystals/PVA nanocomposites membranes. *Journal of industrial and engineering chemistry* **2018**, *57*, 113−124.
(73) Sultana, T.; Sultana, S.; Nur, H. P.; Khan, M. W. Studies on mechanical, thermal and morphological properties of betel nut husk nano cellulose reinforced biodegradable polymer composites. *Journal of Composites Science* **2020**, *4* (3), 83.
(74) Phanthong, P.; Reubroycharoen, P.; Kongparakul, S.; Samart, C.; Wang, Z.; Hao, X.; Abudula, A.; Guan, G. Fabrication and evaluation of nanocellulose sponge for oil/water separation. *Carbohydr. Polym.* **2018**, *190*, 184−9.
(75) Goudar, N.; Vanjeri, V. N.; Dixit, S.; Hiremani, V.; Sataraddi, S.; Gasti, T.; Vootla, S. K.; Masti, S. P.; Chougale, R. B. Evaluation of multifunctional properties of gallic acid crosslinked poly (vinyl alcohol)/tragacanth gum blend films for food packaging applications. *Inter j biologmacromol* **2020**, *158*, 139−149.
(76) Zhang, C. J.; Wang, L.; Zhao, J. C.; Zhu, P. Effect of drying methods on structure and mechanical properties of bacterial cellulose films. *Adv. Mater. Research* **2011**, *239-242*, 2667−2670.
(77) Cazier, J. B.; Gekas, V. Water activity and its prediction: a review. *Int. J. Food Prop* **2001**, *4*, 35−43.
(78) Yang, L.; Zhang, H. Y.; Yang, Q.; Lu, D. N. Bacterial cellulose−poly (vinyl alcohol) nanocomposite hydrogels prepared by chemical crosslinking. *J. of AppldPolym. Sci.* **2012**, *126* (S1), E245−E251.
(79) Yang, L.; Wang, C.; Chen, L.; Wang, X.; Cui, P.; Zhang, T. Effect of aldehydes crosslinkers on properties of bacterial cellulose-poly (vinyl alcohol)(BC/PVA) nanocomposite hydrogels. *Fibers Polym.* **2017**, *18* (1), 33−40.
(80) Wang, M.; Miao, X.; Li, H.; Chen, C. Effect of Length of Cellulose Nanofibers on Mechanical Reinforcement of Polyvinyl Alcohol. *Polym.* **2022**, *14* (1), 128.
(81) Peng, H.; Wang, S.; Xu, H.; Hao, X. Preparation, properties and formation mechanism of cellulose/polyvinyl alcohol bio-composite hydrogel membranes. *New J. Chem.* **2017**, *41* (14), 6564−73.
(82) Haghighi, H.; Gullo, M.; La China, S.; Pfeifer, F.; Siesler, H. W.; Licciardello, F.; Pulvirenti, A. Characterization of bio-nano-

https://doi.org/10.1021/acsomega.2c04336
ACS Omega 2022, 7, 43559−43573

composite films based on gelatin/polyvinyl alcohol blend reinforced with bacterial cellulose nanowhiskers for food packaging applications. *Food Hydrocolloids* **2021**, *113*, 106454.
(83) Bagewadi, Z. K.; Dsouza, V.; Mulla, S. I.; Deshpande, S.H.; Muddapur, U. M.; Yaraguppi, D. A.; Reddy, V. D.; havikatti, J. S.; More, S. S. Structural and functional characterization of bacterial cellulose from Enterobacter hormaechei subsp. steigerwaltii strain ZKE7. *Cellulose* **2020**, *27* (16), 9181−9199.
(84) Slavutsky, A. M.; Bertuzzi, M. A. Water barrier properties of starch films reinforced with cellulose nanocrystals obtained from sugarcane bagasse. *Carbohydpolym* **2014**, *110*, 53−61.
(85) Ben Halima, N. Poly (vinyl alcohol): review of its promising applications and insights into biodegradation. *RSC adv* **2016**, *6* (46), 39823−39832.
(86) Tan, B. K.; Ching, Y. C.; Poh, S. C.; Abdullah, L. C.; Gan, S. N. A review of natural fiber reinforced poly (vinyl alcohol) based composites: Application and opportunity. *Polymers* **2015**, *7* (11), 2205−2222.
(87) Stoica-Guzun, A.; Jecu, L.; Gheorghe, A.; Raut, I.; Stroescu, M.; Ghiurea, M.; Danila, M.; Jipa, I.; Fruth, V. Biodegradation of poly (vinyl alcohol) and bacterial cellulose composites by Aspergillus niger. *Journal of Polymers and the Environment* **2011**, *19* (1), 69−79.
(88) Zahan, K. A.; Azizul, N. M.; Mustapha, M.; Tong, W. Y.; Rahman, M. S. A. Application of bacterial cellulose film as a biodegradable and antimicrobial packaging material. *Materials Today: Proceedings.* **2020**, *31*, 83−88.
(89) Jayasekara, R.; Harding, I.; Bowater, I.; Lonergan, G. Biodegradability of a selected range of polymers and polymer blends and standard methods for assessment of biodegradation. *Journal of Polymers and the Environment* **2005**, *13* (3), 231−51.
(90) Chiellini, E.; Corti, A.; D'Antone, S.; Solaro, R. Biodegradation of poly (vinyl alcohol) based materials. *Progress in Polymer science* **2003**, *28* (6), 963−1014.

https://doi.org/10.1021/acsomega.2c04336
ACS Omega 2022, 7, 43559−43573